Study of CZTS morphology grown by immersion and sulfurization

Cite as: AIP Conference Proceedings **2320**, 030009 (2021); https://doi.org/10.1063/5.0037824
Published Online: 02 March 2021

Fianti, Wening Nurul Amaliyah, Aulia Rosi Kusuma Wardani, Ngurah Made Darma Putra, Triastuti Sulistyaningsih, Sulhadi, and Putut Marwoto

Study of Czts Morphology Grown by Immersion and Sulfurization

Fianti[1], Wening Nurul Amaliyah[1,a)], Aulia Rosi Kusuma Wardani[1], Ngurah Made Darma Putra[1], Triastuti Sulistyaningsih[1], Sulhadi[1], and Putut Marwoto[1]

[1]*Jurusan Fisika, Fakultas Matematika dan Ilmu Pengetahuan Alam, Universitas Negeri Semarang (UNNES), Jl. Raya Sekaran, Gunungpati, Semarang Indonesia 50029*

[a)]Corresponding author: weningnurul97@gmail.com

Abstract. Cu_2ZnSnS_4 (CZTS) thin films were developed for safe and inexpensive thin films. The research aims to provide detailed information about the morphology of CZTS grown by immersion and sulfurization techniques on soda-lime glass (SLG) and indium tin oxide (ITO). CZTS thin films were prepared in two stages, i.e., CZTS precursors were prepared by substrate immersion in precursor solution firstly and then sulfurization in a furnace with sulfur pellet addition and heat treatment (540 °C for 30 minutes). The CZTS thin films were characterized by XRD, SEM-EDX, and completed by Smartphone and CCD cameras for larger area observation. The EDX test produces Cu-poor and Zn-rich films. The structure of kesterite crystals and amorphous CZTS thin films on SLG and ITO substrates was identified through XRD characterization results. The sequential thickness of films from SLG A's film, SLG B's film, SLG C's film, ITO A's film, ITO B's film, ITO C's film is 11.64 μm, 9.33 μm, 17 μm, 11.96 μm, 3.64 μm, 62.08 μm. CZTS thin-film morphologies observed by using Smartphone camera, CCD, and SEM were showed that there were cracks and voids yielding inhomogeneous grains and high porosity thin films. The comparison revealed that the thin films grown on ITO showed smaller cracks and higher homogeneity than that on SLG.

INTRODUCTION

Crude oil is the most important source of energy in global terms. Around 35% of the world's main energy consumption is supplied by oil [1]. The risk of high oil production is that oil spills are a major problem of environmental pollution. The threat of climate change, greenhouse gases, and the problem of oil drilling can disrupt terrestrial and marine ecosystems. This makes the demand for environmentally friendly energy resources continue to increase, as one solution to overcome the problem of petroleum.

Of all renewable sources, solar energy has the highest potential, with /a potential equivalent to 23,000 TW with an energy potential received by the earth of 174 PW [1-3]. The high potential of solar energy is used as solar cells. Solar cells are a method for converting solar energy into electricity using semiconductor materials that exhibit photovoltaic effects (creating voltage differences in materials after exposure to light) [4].

At present, commercial thin-film solar cell technology is dominated by cadmium telluride (CdTe) and $CuIn_xGa_{(1-x)}Se_2$ (CIGS) as *p*-type semiconductors [5]. However, In and Ga are rare elements and their use is limited due to unlimited abundance, large-scale commercialization at the industrial level. In contrast, Cd and Te are highly toxic; ; due to this shortage, many researchers have found alternative absorbers for In and Ga film solar cell films thin CIGS-based, with an abundance of elements that are large and non-toxic [6]. Semiconductor CZTS has emerged as a new type of potential absorber material for large scale production of solar cells. This type of semiconductor solar cell consists of abundant non-toxic elements. Optical energy of 1.0 - 1.5 eV and a high absorption coefficient of 104 cm^{-1} have attracted the manufacture of thin-film solar cells [7].

The growth of CZTS crystalline thin-film solar cells with immersion and sulfurization techniques was carried out at annealing temperature of 540 ºC, annealing at temperatures above the boiling point around 440 ºC so that the sulfur evaporates and chemical reactions occur with the film, by optimizing the concentration of Cu in the solution

The 9th National Physics Seminar 2020
AIP Conf. Proc. 2320, 030009-1–030009-7; https://doi.org/10.1063/5.0037824
Published by AIP Publishing. 978-0-7354-4064-7/$30.00

CZTS to get the best precursor [8]. Previous researchers have succeeded in preparing CZTS on SLG substrates and in ITO [2,9]. The success of previous studies provided an opportunity to examine the morphology of SLG and ITO substrates. Moreover, this research provided information for further research, i.e., comparing in using two kinds of substrates and Cu controlling to achieved better morphology, crystals structures, and balance composition.

METHOD

Substrate Preparation

SLG and ITO substrate preparation includes cutting, washing, and drying. The substrate was cut to a size of 1.5 x 1.5 cm. The substrate was washed using acetone, ethanol, and deionized water in an ultrasonic cleaner 10 minutes each, then dried with nitrogen gas. Then, one side of substrate surfaces was tape-covered using tweezers and other surfaces left without tape-covered.

Precursors Preparation

Preparation of precursors begun with weighing the ingredients for precursor solutions consisting of (Cu+Zn+Sn) with composition variations of Cu/(Zn + Sn). Zn/Sn composition was fixed. After the ingredients were weighed, they were mixed well by in the beaker over the magnetic stirrer, which has been set at 160 ^{o}C. Furthermore, mixing $CuCl_2.2H_2O$, $SnCl_2.2H_2O$, and $ZnCl_2$ with ethanol as a solvent using a magnetic stirrer at 160 ^{o}C for 15 minutes. The precursors were aged for 5 minutes, then thiourea was added and stirred again for 5 minutes at 160 ^{o}C.

Thin Film Deposition

CZTS thin film deposition using the immersion technique, this method was done by dipping the substrate into the CZTS precursor for 20 minutes which is then drained for 30 minutes before the drying process. Before the film was dried, the tape sticking to one of the surfaces was removed using tweezers.

Drying Thin Films

The film was dried by heating it on a magnetic stirrer using a petri dish which was covered by the aluminum foil for 30 minutes at 50 ^{o}C.

CZTS Thin Film Growth

The growth of CZTS thin films was carried out in furnace by the sulfurization technique and adding sulfur pellets in closed ampoule near the precursor films at 540 ^{o}C for 30 minutes.

RESULTS AND DISCUSSION

The growth of CZTS thin films with Cu control applied to different substrates has been successfully carried out. The results of growing thin films were showed in the following data. Deposited elements on the substrate can be seen in Figure 1 from EDS.

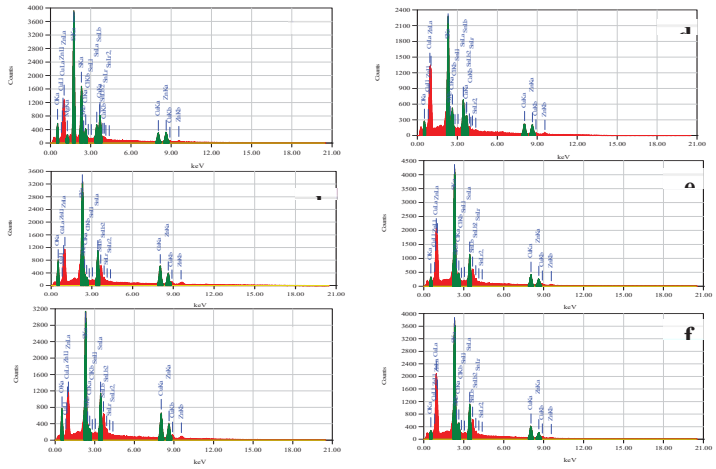

FIGURE 1. EDS Graph (a) SLG A film, (b) SLG B film, (c) SLG C film, (d) ITO A film, (e) ITO B film, (f) ITO C film.

In the EDS chart above, Cu-Zn-Sn-S elements were identified as CZTS compositions. Besides Cu-Zn-Sn-S, other elements were identified such as O, Mg, Ca, Si, and Cl. The elements O, Mg, Ca, and Si themselves were elements of SLG which were formed from SiO_2, CaO, and MgO compounds [10]. Cl came from an un-evaporated compound of the precursor solution in the form of XCl_2.

TABLE 1. CZTS precursor composition

	$CuCl_2$ (mmol)	$ZnCl_2$ (mmol)	$SnCl_2$ (mmol)	CH_4N_2S (mmol)
Film SLG A	5.9	10.9	9	80
Film SLG B	8.8	10.9	9	80
Film SLG C	13.2	10.9	9	80
Film ITO A	5.9	10.9	9	80
Film ITO B	8.8	10.9	9	80
Film ITO C	13.2	10.9	9	80

TABLE 2. CZTS composition after annealing

	Cu (at.%)	Zn (at.%)	Sn (at.%)	S (at.%)	Cu/(Zn+Sn)	Zn/Sn
Film SLG A	22.82	28.82	9.62	38.74	0.59	3.00
Film SLG B	29.02	19.95	12.29	38.74	0.90	1.62
Film SLG C	29.51	19.88	12.81	37.80	0.90	1.55
Film ITO A	25.58	28.52	11.26	34.64	0.64	2.53
Film ITO B	27.66	21.57	11.35	39.42	0.84	1.90
Film ITO C	30.51	18.61	12.73	38.15	0.97	1.46

The ingredients of precursor solution can be seen in Table 1 that referred to a research conducted by Munir (2015), the Zn/Sn composition ratio was 1.2 to get the Zn-rich ratio [11]. Here, thiourea provided S in the precursor solution. The Cu elements in Table 1 were used a little, but the results after annealing showed quite a high composition, with the addition of S from thiourea Cu oxidation become stable [12]. The following was the mechanism of the Cu_2ZnSnS_4 compounds formation with their formation temperatures [13]:

- $2Cu + S \rightarrow Cu_2S$ (< 300–350 °C)
- $Zn + S \rightarrow ZnS$ (< 300–350 °C)
- $Sn + 2S \rightarrow SnS_2$ (< 300–350 °C)
- $Cu_2S + SnS_2 \rightarrow Cu_2SnS_3$ (>350–400 °C)
- $Cu_2SnS_3 + ZnS \rightarrow Cu_2ZnSnS_4$ (>350–500 °C).

Based on the EDS CZTS results, the composition of Cu in precursor solution (Table 1) caused the Cu/(Zn+Sn) variation, a way to approach the ideal ratio of Cu-poor and Zn-rich, Table 2, for having *p*-type semiconductor. The ratio of the ideal composition of Cu-poor CZTS Cu/(Zn+Sn) and Zn/Sn was 0.75-0.95 and 1.1-1.4 [14]. The EDS results show that SLG A and ITO A films (with the lowest Cu concentrations) are far from ideal Cu-poor conditions, both films lack of Cu with exceeding of Zn in a range of Cu-poor 0-75-0.95 and Zn-rich 1.1-1.4, in the range Cu/Zn+Sn < 0.75 and Zn/Sn > 1.4. SLG C and ITO C films (with the highest Cu concentrations in films) approached the desired ratio. Moreover, low sulfurization pressure will induce the S-poor state in CZTS thin films, while high sulfurization pressure can increase the growth of CZTS thin films [15].

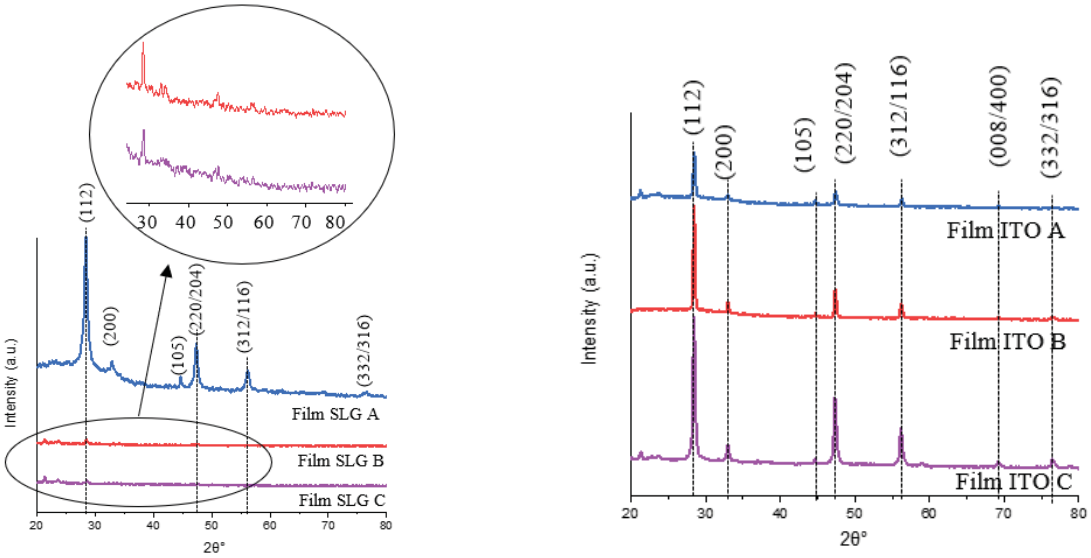

(a) (b)

FIGURE 2. XRD results (a) on SLG, (b) on ITO

The XRD results on SLG A film showed the kesterite phase based on COD 96-900-4751, the kesterite phase has seen at the peak (220/204) and (312/116) overlapping each other into one peak. Whereas, SLG B and SLG C films showed peaks only at 28.5 °2θ. The kesterite phase tended to appear than the stannite phase because the stannite phase was less thermodynamically stable than the kesterite phase, so the stannite phase was rarely formed on the CZTS thin film [16]. Also, the SLG substrate had a high concentration of Na^+; Na^+ concentration interfered with the diffusion of Cu in thin films inhibiting the process of film growth [17]. All ITO films showed a kesterite phase based on COD 96-900-4751 at peaks (112), (220/204), (312/116) along with weak peaks (200), (105), (008/400), (332/316).

The morphology of CZTS thin films applied to different substrates was showed in data using smartphones, CCD, and SEM cameras. Thin-film morphology displayed using a Smartphone camera with a substrate size of 1.5 cm x 1.5 cm on SLG and ITO substrates.

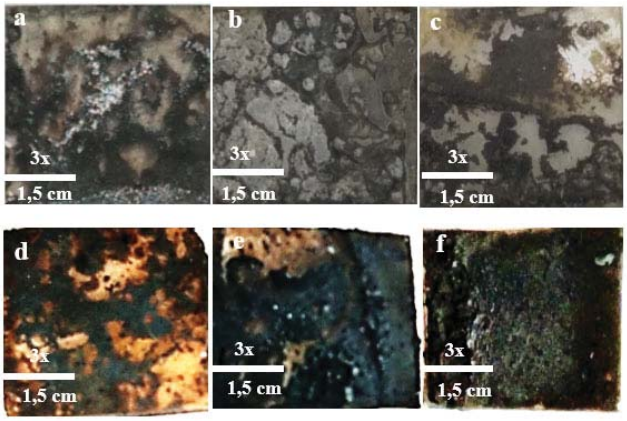

FIGURE 3. Smartphone Camera (a) SLG A film, (b) SLG B film, (c) SLG C film, (d) ITO A film, (e) ITO B film, (f) ITO C film.

The morphologies showed in thin films on SLG and ITO substrates shows that the most homogeneous surface was shown in Figure 3(f), which was Cu 13.2 mmol on ITO. While thin-film surfaces in Figure 3(a), 3(c), and 3(e) showed bad morphologies because the surface was inhomogeneous. The morphology of the film at ITO showed that the morphology and adhesivity were better indicated by voids and cracks smaller than the film on SLG, this different maybe because of the more effective adhesion of thiourea metal gel complex with ITO substrate than SLG [18].

Thin-film morphology on SLG and ITO substrates displayed using a charge-coupled device (CCD) at a magnification of 1800 times with an area length of 150 μm. The observation results showed that the best film was obtained on SLG C film with rather homogeneous and a little cracked. SLG A films and SLG B films showed no cracks on the film but inhomogeneous grains from its non-flat film surface. All films look homogeneous; there were only cracks in all films. The CCD results showed that the more Cu that was used, the less cracked in the film.

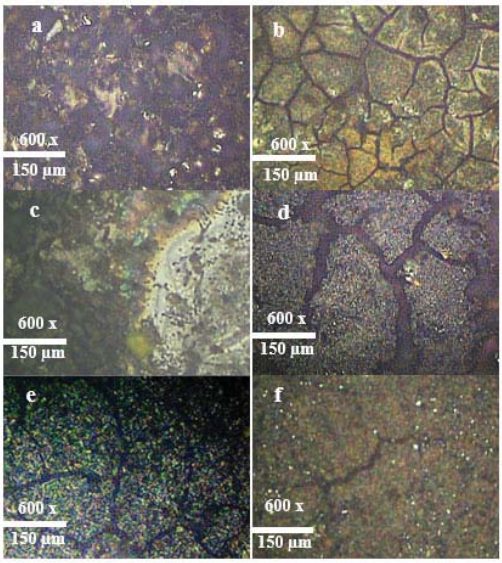

FIGURE 4. CCD (a) SLG A film, (b) ITO A film, (c) SLG B film, (d) ITO A film, (e) SLG C film, (f) ITO C film.

Thin-film morphology on SLG and ITO substrates displayed using a 5,000 times magnification of Scanning Electron Microscope (SEM) with an area of 5 x 5 μm^2, Figure 5. All films showed inhomogeneous grains and much porosity in the film. Porosity and cracks were clearly seen in films c and e. This was because of the carbon composition of precursor solution decomposed to form a gas phase leaving a path in the film before finally freed and arrived at the surface [2]. SEM images showed that the most homogeneous films were ITO C films. In addition, films on ITO showed better adhesivity and morphology than films on SLG.

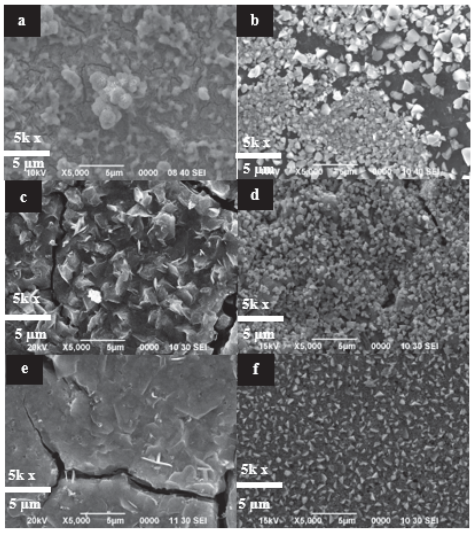

FIGURE 5. SEM (a) SLG A film, (b) ITO A film, (c) SLG B film, (d) ITO A film, (e) SLG C film, (f) ITO C film.

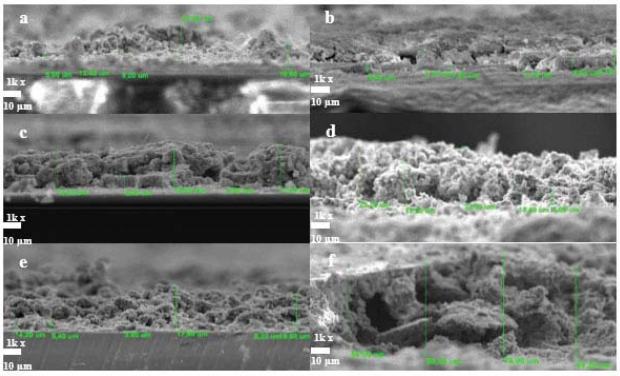

FIGURE 6. Cross section (a) SLG A film, (b) ITO A film, (c) SLG film B, (d) ITO A film, (e) SLG C film, (f) ITO C film.

TABLE 3. Thickness of Thin Film CZTS

	Thickness (μm)
Film SLG A	11.62
Film SLG B	11.96
Film SLG C	9.33
Film ITO A	3.64
Film ITO B	17.00
Film ITO C	62.08

Thickness results based on data from consecutive cross-sections of a-e are shown in Figure 6 and Table 3. The cross-section of the film was based on SEM observation. The surface of the film was not flat with cavities. According to Jhuma et al. (2019), the optimum thickness of CZTS in the range of 100-2000 nm. On the other hand, all prepared films have not met the criteria as a good absorber layer because the thickness was more than 2000 nm [19], which lead to poor adhesivity of thin film on a substrate caused by the increasing of film thickness [20].

CONCLUSIONS

CZTS thin films were developed as a safe and low-cost alternative. This study aims were to grow and provide thin film properties and then compare the morphologies of CZTS thin films grown with immersion and sulfurization techniques onto SLG and ITO substrates. The growth of CZTS films with immersion and sulfurization was successfully on SLG and ITO substrates, which were Cu-poor and Zn-rich. CZTS structure was kesterite. The morphology of the CZTS thin film observed from smartphones, CCD, and SEM showed cracks and voids so that the porosity of the film was large. More film cracks were observed on SLG, contrary, films on ITO showed flat and better homogeneity.

ACKNOWLEDGEMENT

This research has been supported by Dana DIPA FMIPA UNNES 2020.

REFERENCES

1. V. Smil, *Energy in Nature and Society: General Energetics of Complex Systems*, (MIT Press, London, 2008).
2. B. Munir, B. E. Prastyo, E. Y. Muslih and D. M. Nurjaya, *International Journal of Technology* **8**, pp. 1326–1334, (2016).
3. R. Perez and M. Perez, *The IEA SHC Solar Update* **50** (April), pp. 1–12, (2009).
4. V. Cingoski and B. Petrevska, *Journal of Applied Economics and Business* **5** (4), pp. 1–103, (2017)
5. B. Parida, S. Iniyan and R. Goic, *A Review of Solar Photovoltaic Technologies. Renewable and Sustainable Energy Reviews* **15** (3), pp. 1625–1636, (2011).

6. S. Adachi, *Earth-Abundant Materials for Solar Cells : Cu_2-II-IV-VI_4 Semiconductors (first)*. (John Wiley & Sons Ltd., West Sussex, 2015).
7. C. Persson, *Journal of Applied Physics* **107** (5), 053710, (2010).
8. A. Setiawan, *Rekayasa dan Manajemen Transportasi* **2** (1), pp. 22–33, (2013)..
9. A. Ashfaq, J. Jacob, N. Bano, M. A. U. Nabi, A. Ali, W. Ahmad, K. Mahmood, M. I. Arshad, S. Ikram, U. Rehman, N. Amin and S. Hussain, *Ceramics International* **45** (8), pp. 10876–10881, (2019).
10. R. Kurniawan, *Konversi* **7**(1), (2018).
11. B. Munir, B. E. Prastyo, D. M. Nurjaya, E. Y. Muslih and S. K. Alfauzan, *AIP Conference Proceedings* **1788**, (2017).
12. D. K. Maurya, S. Sirkawar, P. Chaundhary, S. Angaiah and B. C. Yadav, *IEEE Sensor Journal* **19** (4), pp. 2837-2846, (2019).
13. P. Reith and H. Gerben, "Investigating electrodeposition to grow CATS thin film for solar cell applicatipons", disertation, University of Minnesota, (2012).
14. M. P. Suryawanshi, U. V. Ghorpade, U. P.,Suryawanshi, M. He, J. Kim, M. G. Gang and J. H Kim, *ACS Omega* **2** (12), pp. 9211–9220, (2017).
15. H. Cai, Y. Xia, C. Dao, J. Li, L. Lin, X. Kong, S. Chen, Z. Huang and G. Chen, *ACS Applied Energy Materials* **2**(10), pp. 7279–7287, (2019).
16. A. Ziti, B. Hartiti, H. Labrim, S. Fadili, A. Batan, M. Tahri, M. Ridah, O. Mounkachi, A. Benyoussef and P. Thevenin, *Journal of Materials Science: Materials in Electronics*, **30** (14), pp. 13134–13143, (2019).
17. A. R. Jeong, W. Jo, D. Y. Park, H. Cheong, Y. K. Seo, J. H. Park, J. S. Chung, Y. S. Lee and Y. J. Kwark, *Current Applied Physics* **13** (5), pp. 907–912, (2013).
18. S. Kumar, B. Kasubosula, M. Loorits, J. Raudoja, V. Mikli, M. Altosaar and M. Grossberg, *Energy Procedia* **102** (5), pp. 102–109, (2016).
19. F. A. Jhuma, M. Z. Shaily and M. J. Rashid, *Materials for Renewable and Sustainable Energy* **8** (1), pp. 1–7, (2019).
20. T. Atwee, A. S. Gadallah, M. A. Salim and A. M. Ghander, *Applied Physics A: Materials Science and Processing* **125** (4), pp. 1–10, (2019).